Bifurcation analysis of a semiconductor laser subject to non-instantaneous phase-conjugate feedback

Kirk Green and Bernd Krauskopf

Department of Engineering Mathematics, University of Bristol, Bristol BS8 1TR, UK

ABSTRACT

We study the behaviour of a semiconductor laser subject to phase-conjugate feedback when the interaction time of the phase-conjugating mirror changes. With continuation techniques we present two-parameter bifurcation diagrams in the plane of feedback strength versus pump current, which change qualitatively as the interaction time of the mirror is increased. This reveals that for small interaction times the assumption of instantaneous feedback is justified. On the other hand, increasingly larger interaction times lead to considerable changes in the locking region. By investigating how curves of Hopf bifurcations change with the interaction time, we show how more complicated, chaotic dynamics become suppressed. One-parameter bifurcation diagrams as a function of the pump current, obtained by simulation, complement the continuation analysis.

Keywords: Semiconductor lasers, non-instantaneous phase-conjugate optical feedback, locked steady state operation, bifurcation analysis

1. INTRODUCTION

In this paper we investigate a semiconductor laser receiving phase-conjugate feedback (PCF) from a phase-conjugating mirror (PCM). In contrast to conventional optical feedback (COF) from a regular mirror, during PCF the phase of the light is reversed at the PCM. The return conjugated wave travels back along the exact path as the incident wave. This has a number of advantages; for example, any perturbations of the laser light between the laser and the external mirror are cancelled out on the return trip, so that the PCF laser system is self-aligning. This results in a extremely narrow and highly-focused beam[1–3] that can be used for mode-locking and phase-locking.[4] Furthermore, the PCF laser has been shown to produce a plethora of interesting nonlinear dynamics, including periodic oscillations, quasiperiodic modulations and chaotic operation.[5–9]

Modelled mathematically by Lang-Kobayashi[10] type delay differential equations (DDE),[11–13] the feedback from the PCM is normally assumed to respond instantaneously. However, in reality this is not the case as there is always an interaction time as the phase-conjugated wave is generated within the PCM. Interaction times can be extremely fast; for example, femtosecond to picosecond responses from four-wave mixing (FWM) in a Kerr-like nonlinear medium, such as, a semiconductor material with counter-propagating pump beams.[14] However, PCF formed in a photo-reactive crystal or an atomic vapour may have an interaction time of nanoseconds.[15] Consequently, an investigation of the effect of a varying PCM interaction time on the dynamics of the PCF laser is important. Specifically, the question remains: Does the instantaneous PCF model describe the dynamics of the PCF laser sufficiently well?

To answer this question, we derive and consider a DDE model describing a semiconductor laser subject to non-instantaneous PCF. We then use advanced numerical tools, namely the continuation package DDE-BIFTOOL[16] to investigate how the two-parameter bifurcation diagram of the locked steady state solution, in the plane of feedback strength versus pump current, changes qualitatively with the increasing PCM interaction time. We show that the bifurcation diagram for small PCM interaction times shows qualitatively little change to that presented in Ref. [9] for instantaneous PCF. Furthermore, we show how the chaotic dynamics are suppressed for higher interaction times, which is due to a qualitative change of regions in the parameter plane that are bounded by curves of Hopf bifurcations. Our results are reinforced by considering one-parameter bifurcation diagrams obtained by numerical simulation showing transitions through the parameter plane for fixed feedback strength and varying pump current.

E-mail addresses: Kirk.Green@bristol.ac.uk, B.Krauskopf@bristol.ac.uk

symbol	meaning	value
α	linewidth enhancement factor	3
G_N	optical gain	1190 s^{-1}
N_0	transparency electron number	1.64×10^8
τ_p	photon lifetime	1.4×10^{-12} s
ϵ	nonlinear gain coefficient	3.57×10^{-8}
κ	feedback rate	variable
τ	external cavity round-trip time	$(2/3) \times 10^{-9}$ s
I	pump current	variable
q	electron charge	1.6×10^{-19} C
τ_e	electron lifetime	2.0×10^{-9} s

Table 1: Parameters of Eqs. (1)–(2).

2. RATE EQUATIONS

A single-mode semiconductor laser subject to PCF can be described by the rate equations

$$\frac{dE}{dt} = \frac{1}{2}\left[-i\alpha G_N(N(t) - N_{\mathrm{sol}}) + \left(G(t) - \frac{1}{\tau_p}\right)\right] E(t) + \kappa F(t,\tau), \tag{1}$$

$$\frac{dN}{dt} = \frac{I}{q} - \frac{N(t)}{\tau_e} - G(t)\,|E(t)|^2 \tag{2}$$

for the evolution of the slowly varying complex electric field $E(t)$ and the population inversion $N(t)$. Nonlinear gain is included as $G(t) = G_N(N(t) - N_0(1 - \epsilon P(t)))$, where $P(t) = |E(t)|^2$ is the intensity. Furthermore, $N_{\mathrm{sol}} = N_0 + 1/(G_N\tau_p)$. The parameter values we use correspond to a Ga-Al-As semiconductor laser and are given in Table 1.

The feedback term $\kappa F(t,\tau)$ in Eq. (1) involves the feedback rate κ and the round-trip time τ between the laser and the PCM. We fix τ at the realistic value of $\tau = 2/3$ ns, corresponding to an distance between the laser and the PCM of $L_{\mathrm{ext}} \approx 10$ cm. In the two-parameter continuation studies that follow we consider bifurcations in the plane of dimensionless feedback strength $\kappa\tau$ versus pump current I. Furthermore, in the simulations we fix the value of the feedback strength to $\kappa\tau = 5.0$ and consider the dynamics as a function of the free pump current I. Note that both I and $\kappa\tau$ are experimentally accessible parameters.

If the PCM responds instantaneously, the feedback term in Eq. (1) can be written as $F(t,\tau) = E^*(t-\tau)$ (under the assumption of weak feedback). This instantaneous case has received considerable attention.[5–9, 17] A more complicated PCF model is derived in Ref. [14] where a single-Lorentzian approximation for non-instantaneous feedback is given as

$$F(t,\tau) = \frac{1}{t_m}\exp\left[-2i\delta_0(t-\tau/2)\right] \cdot \int_{-\infty}^{t} E^*(t'-\tau)\exp\left[-\frac{(1-i\delta_0 t_m)(t-t')}{t_m}\right] dt' \,,$$

where the interaction time t_m is related to the effective depth or length of the PCM.[14] The parameter δ_0 corresponds to a detuning from the pump laser used for FWM. As is common in the field, and for mathematical simplicity, we set $\delta_0 = 0$. For studies of how variations in δ_0 affect the dynamics of the PCF laser see Refs. [18, 19].

In Ref. [14] the authors used a recurrence relation to solve the integral equation for $F(t,\tau)$, above. Here we differentiate with respect to time to obtain the differential equation

$$\frac{dF}{dt} = \frac{1}{t_m}\left(E^*(t-\tau)\exp\left[-2i\delta_0(t-\tau/2)\right] - (1-i\delta_0 t_m)F(t)\right) \tag{3}$$

for the complex feedback field $F(t)$. This approach avoids approximation of the feedback term, and it is directly suitable for numerical continuation techniques. Note that in Eq. (3), as $t_m \to 0$, we recover the equation for instantaneous PCF because $F(t,\tau) \to E^*(t-\tau)$.

Therefore, the semiconductor laser subject to PCF from a non-instantaneous PCM is described by Eqs. (1)–(3). Like those describing an instantaneously responding PCM, these equations have $\mathbb{Z}_2$-symmetry under the transformation $(E, F, N) \to (-E, -F, N)$. The symmetry group is $\mathbb{Z}_2 = \{1, -1\}$, corresponding to rotations over π of the complex E and F planes. Physically, this corresponds to a phase shift by π of the electric field.[20]

3. TWO-PARAMETER BIFURCATION DIAGRAMS

Figure 1 shows bifurcations of the locked steady state solution of the PCF laser in the plane of feedback strength $\kappa\tau$ versus pump current I. The individual panels of Fig. 1 present qualitatively different two-parameter bifurcation diagrams for different representative values of the PCM interaction time t_m. The shaded areas represent regions of the parameter plane in which the steady state solution is stable, this is called the *locking region* of the PCF laser.[9] Physically, this locked solution corresponds to a frequency match between the solitary laser and the pump lasers used in the FWM process.[21]

In each panel of Fig. 1, the locking region is bounded to the left by a curve of saddle-node bifurcations S. This instability is responsible for the birth of the stable locked solution seen to the right of the curve S, as well as an unstable saddle steady state. The locking region is bounded from below by a curve of Pitchfork bifurcations P. This instability marks the onset of lasing, that is, below the curve P the PCF laser is in its 'off-state' and it is 'on' above the curve P. Inside the region bounded by the curves S and P the PCF laser can undergo stable locked operation. However, as is shown in Fig. 1, this stable operation is destabilised at curves of Hopf bifurcations $H_{1,2,3}$, marking the onset of oscillatory instabilities in the laser light. The Hopf curves are drawn dark when they are supercritical, that is, the bifurcating periodic solution is stable; they are drawn light when they are subcritical, that is, the bifurcating periodic solution is unstable.

Each panel of Fig. 1 was chosen to show a qualitatively different bifurcation diagram as the PCM interaction time t_m varies. Figure 1(a) shows that for $t_m = 0.1$ ns the stable locked steady state solution born at the curve S is destabilised for increasing feedback strength $\kappa\tau$ in a Hopf bifurcation. For large values of the pump current I stability is lost at the curve of supercritical Hopf bifurcations H_3. Whereas, for intermediate values of the pump current I stability is lost at the curve of supercritical Hopf bifurcations H_2. The curves H_2 and H_3 cross at a codimension-two double-Hopf point D. For low values of the pump current I the situation is slightly different. In this case, the stable locked steady state solution is destabilised at the Hopf curve H_1 which is supercritical below the point c, yet subcritical between the points c and the crossing of the curves H_1 and H_2 at the double-Hopf point D. In Ref. [7] it was shown that this subcritical Hopf bifurcation H_1 leads to a bistability between the stable locked steady state solution and a periodic solution. The Hopf curve H_1 ends at the codimension-two pitchfork-Hopf bifurcation points PF. Furthermore, Fig. 1(a) shows that for high values of the feedback strength $\kappa\tau$ and low values of the pump current I the PCF laser is shown to lock again. This bifurcation scenario is qualitatively the same as that presented in Ref. [9] for the case of instantaneous PCF. In other words, up to $t_m \approx 0.1$ ns the assumption of instantaneous PCF is justified.

Figure 1(b) for a PCM interaction time of $t_m = 0.3$ ns represents a qualitative change in the interactions of the Hopf curves. Firstly, it is clear that the shaded region of stable locked steady state operation has grown. The three curves of Hopf bifurcations H_1, H_2, and H_3 no longer intersect. In fact, the curve H_2 is closed and the curve H_3 is almost shown to be closed in our parameter region of interest. The curve H_1 still ends at the pitchfork curve P in a pitchfork-Hopf bifurcation PF. The consequence of these isolated curves of Hopf bifurcations is that we now have 'channels' of locking. In other words, one could trace a path through the $(\kappa\tau, I)$-plane, from low values to high values of feedback $\kappa\tau$ without encountering oscillatory behaviour of the PCF laser light, or indeed more complicated dynamics.

As t_m is increased further, Fig. 1(c) for $t_m = 0.6$ ns shows a second qualitative change. The channel of locking between the curves of Hopf bifurcations H_2 and H_3 has disappeared. However, this time the curves H_2 and H_3 do not intersect as in Fig. 1(a) but instead coalesce into a single curve H_{2-3}. This large closed curve consists of entirely supercritical Hopf bifurcations. Furthermore, the curve H_1 has 'lifted-off' from the pitchfork curve P and forms a closed curve of supercritical Hopf bifurcations for low values of the pump current I. Note that the shaded region of stable locked steady state operation has once again grown in size.

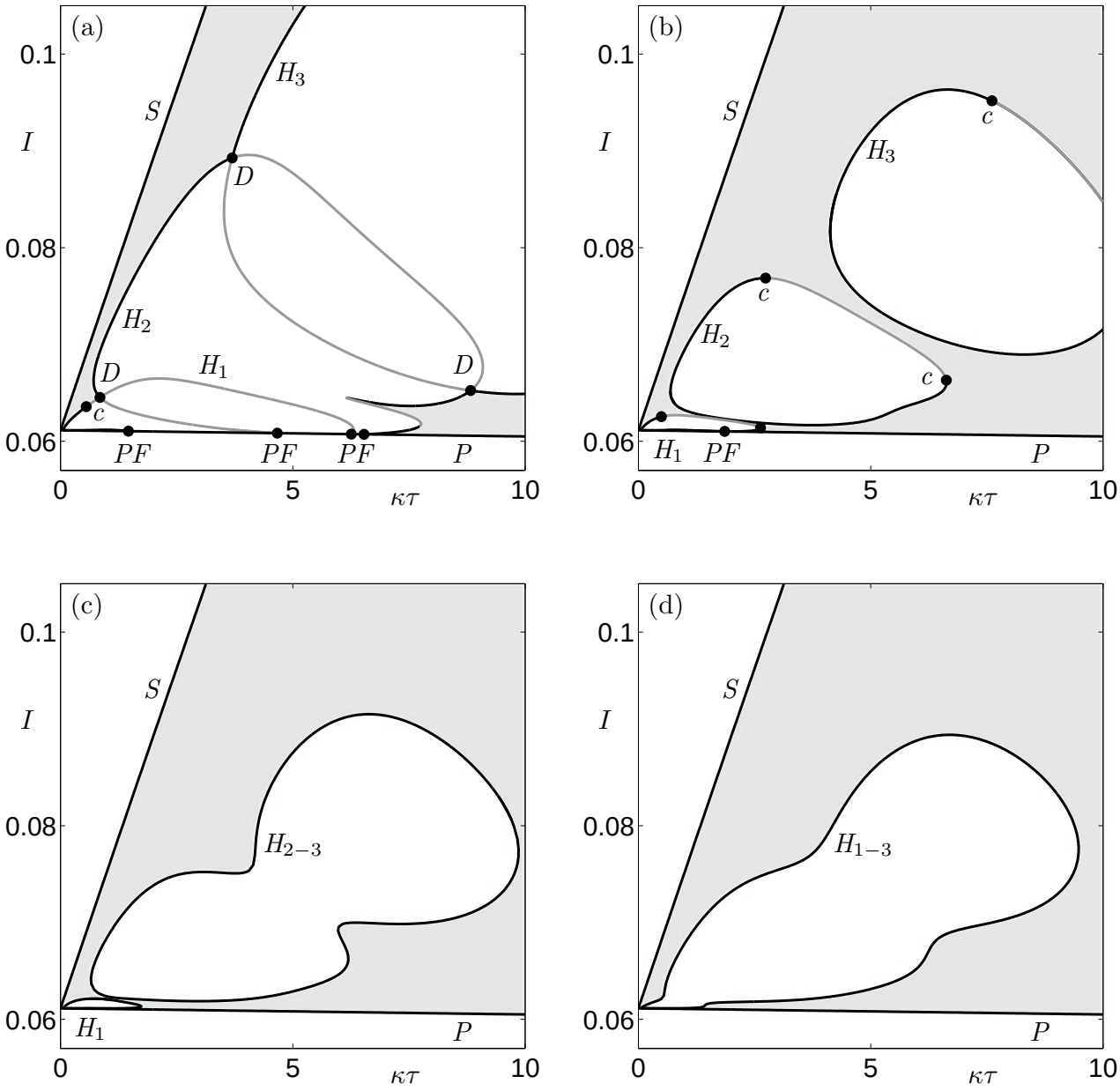

Figure 1. Two-parameter bifurcation diagrams of steady state solutions of the PCF laser in the $(\kappa\tau, I)$-plane. From (a) to (d) the interaction time t_m takes the values 0.1 ns, 0.3 ns, 0.6 ns, and 1.0 ns. The shaded areas correspond to regions in which the steady state solution is stable, that is, the laser is locked.

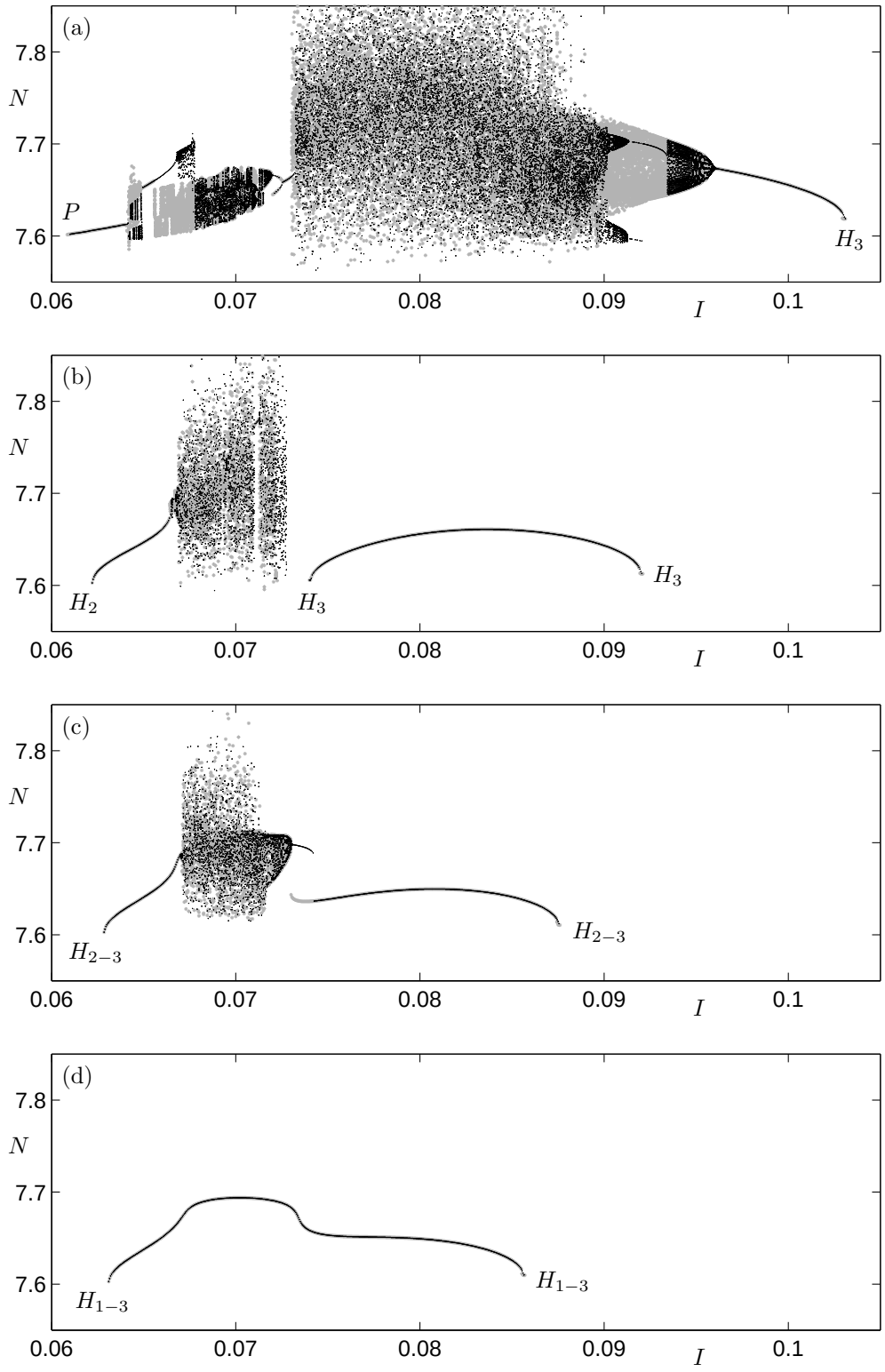

Figure 2. One-parameter bifurcation diagrams obtained by simulation for $\kappa\tau = 5.0$. From (a) to (d) the interaction time t_m takes the values 0.1 ns, 0.3 ns, 0.6 ns, and 1.0 ns. Black dots are computed for increasing and grey dots for decreasing values of the pump current I.

Finally, Fig. 1(d) for $t_m = 1.0$ ns shows that the closed curve H_1 eventually coalesces with the larger curve H_{2-3} to form a single closed curve of supercritical Hopf bifurcations H_{1-3}. In Ref. [22] it is shown that for even higher values of t_m the curve H_{1-3} forms a limiting 'tear-drop' shape. The area of the shaded region of stable locked steady state operation is now at its greatest.

4. ONE PARAMETER TRANSITIONS

We are aware that the bifurcation scenarios described above may be difficult to read for those readers that are less familiar with bifurcation theory. Therefore, we now complement the above analysis by presenting one-parameter transitions, obtained by simulation, through the $(\kappa\tau, I)$-plane for a fixed value of $\kappa\tau$ and varying pump current I.

Figure 2 shows the attracting dynamics of the PCF laser as we take a vertical transition through the two-parameter bifurcation diagrams of Fig. 1 at $\kappa\tau = 5.0$, where t_m increases from panel to panel. By direct numerical simulation of Eqs. (1)–(3), for each value of the pump current I we plot the value of the inversion N whenever the intensity $P(t) = |E(t)|^2$ crosses its average value in the increasing direction. To ensure hysteresis effects are not missed, we compute each transition for increasing I (shown in black) and for decreasing I (shown in grey). Stable steady state dynamics are marked by an absence of points, a small number of points correspond to periodic oscillations, and a large number of points correspond to quasiperiodic or chaotic dynamics of the laser light.

For the small interaction time of $t_m = 0.1$ ns, Fig. 2(a) shows a vertical transition through the bifurcation diagram shown in Fig. 1(a) at $\kappa\tau = 5.0$. For low values of I we observe an absence of points corresponding to the 'off-state' of the PCF laser. A pitchfork bifurcation P at $I \approx 61.0$ mA marks the onset of periodic oscillations. These oscillations then bifurcate to small regions of (almost quasiperiodic) chaotic dynamics. Note the bistability between the attractors for increasing I (black) and those for decreasing I (grey). In terms of Fig. 1(a) we are passing through the areas enclosed by the curves H_1 and H_2. Increasing I further sees a small region of periodic oscillations appear at $I \approx 72.0$ mA followed by a large region of chaos beginning at $I \approx 73.0$ mA. Note that the onset of chaos tallies with crossing the curve H_3 in Fig. 1(a). The main region of chaos ends at $I \approx 89.0$ mA where we observe a bistability between periodic oscillations and quasiperiodic dynamics. A torus bifurcation at $I \approx 96.1$ mA results in periodic oscillations. Finally, at $I \approx 103.1$ mA the periodic solution undergoes a Hopf bifurcation H_3 resulting in a locked steady state solution. This corresponds to the crossing of the upper part of the curve H_3, into the shaded part of Fig. 1(a).

As t_m is increased, Fig. 2(b) for $t_m = 0.3$ ns shows that the second, large region of chaos has disappeared. Specifically, for low values of I we again observe a region of steady state solutions from which emanate periodic oscillations at a Hopf bifurcation H_2 at $I \approx 62.2$ mA. This corresponds to crossing the lower part of the curve H_2 in Fig. 1(b). A small region of chaos is then seen from $I \approx 66.9$ mA to $I \approx 72.7$ mA. This region of chaos ends abruptly and the PCF laser locks again; the 'channel' of locking between the curves H_2 and H_3, shown in Fig. 1(b), has been reached. Finally, a periodic solution is observed to be born in and destroyed in two Hopf bifurcations, the two intersections with the curve H_3. This corresponds to crossing the interior of the curve H_3 shown in Fig. 1(b) before entering the stable locked region at $I \approx 92.0$ mA. Moreover, the bifurcating periodic solution does not undergo further bifurcations.

The chaotic dynamics are shown to diminish further in Fig. 2(c). For $t_m = 0.6$ ns we again observe a stable steady state solution for low values of I which bifurcates to a periodic oscillation at the Hopf bifurcation H_{2-3}; this corresponds to crossing the curve H_{2-3} shown in Fig. 1(c). A small region of chaos is then observed which bifurcates to a quasiperiodic solution and then to a periodic solution. The periodic oscillations then end at the Hopf bifurcation H_{2-3} at $I \approx 87.6$ mA; again, this corresponds to crossing the curve H_{2-3} of Fig. 1(c) before one enters the shaded region of locked steady state dynamics. Note that in Fig. 2(c) we observe a classic hysteresis loop for $I \in [73.0, 74.2]$ mA. For increasing values of I one follows the black solution ending at $I \approx 74.2$ mA, whereas for decreasing I one follows the grey solution ending at $I \approx 73.0$ mA. In between these values of I we observe a bistability between the two periodic solutions.

Finally, Fig. 2(d) for $t_m = 1.0$ ns shows that all chaotic dynamics for $\kappa\tau = 5.0$ have disappeared. A periodic solution is born in a Hopf bifurcation H_{1-3} at $I \approx 63.1$ mA and ends at a Hopf bifurcation H_{1-3} at $I \approx 85.7$ mA. This corresponds to the transition through the Hopf curve H_{1-3} shown in Fig. 2(d). Either side of the Hopf bifurcations H_{1-3} we observe a stable locked steady state operation of the PCF laser. Furthermore, the bifurcating periodic solution does not undergo any further transition.

Taken together, the panels of Fig. 2 show that the interactions of the Hopf bifurcation curves presented in Fig. 1 give a good indication of the complexity of the PCF laser; global qualitative changes in the interaction of the Hopf curves have been shown to be directly related to the suppression of chaotic dynamics in the PCF laser.

5. CONCLUSIONS

We have presented a two-parameter study of the bifurcations of steady state solutions found in a semiconductor laser subject to non-instantaneous PCF. Our analysis revealed that curves of Hopf bifurcations developed into closed curves. The area enclosed by these curves decreased in size as the interaction time of the PCM was increased. Subsequently, the region of locked steady state operation found outside these curves was shown to increase in size. As the curves of Hopf bifurcations interacted with one another, channels of steady state operation between high and low values of feedback strength were shown to open up; these channels may be large enough to observe experimentally.

The periodic solutions born in these Hopf bifurcations are those which undergo bifurcations to chaos; this was observed by direct numerical simulation. As the areas enclosed by the Hopf curves decreased, the regions of chaos of the PCF laser were shown to diminish. An analysis of the bifurcations of the periodic solutions with numerical continuation would shed even greater light on the suppression of the chaotic dynamics. However, the numerical tools needed for such an analysis are not available at present.

Finally, we raise some questions as to the physical cause of a suppression in the chaotic dynamics. Could the reflected field be 'smoothed out' by the finite interaction time of the PCM? In other words, the longer the interaction time, the less coherent the incoming field is to the reflected field. A further effect that needs to be considered is the spectral filtering of the PCM. To this end, PCF could be compared with filtered optical feedback (FOF). Mathematically, the PCF laser is described by equations very similar to the FOF laser and a comparison between the two models would be interesting work for the future.

REFERENCES

1. C. R. Giuliano, "Applications of optical phase conjugation," *Physics Today* **34**, pp. 27–35, April 1981.
2. P. Kurz and T. Mukai, "Frequency stablization of a semiconductor laser by external phase conjugate feedback," *Opt. Lett.* **21**, pp. 1369–1371, 1996.
3. M. Ohstu, I. Koshiishi, and Y. Teramachi, "A semiconductor laser as a stable phase conjugate mirror for linewidth reduction of another semiconductor laser," *Jpn. J. Appl. Phys.* **29**, pp. 2060–2062, 1990.
4. G. R. Gray, D. H. DeTienne, and G. P. Agrawal, "Mode locking in semiconductor lasers by phase-conjugate optical feedback," *Opt. Lett.* **20**, pp. 1295–1297, 1995.
5. B. Krauskopf, G. R. Gray, and D. Lenstra, "Semiconductor laser with phase-conjugate feedback: Dynamics and bifurcations," *Phys. Rev. E* **58**, pp. 7190–7196, 1998.
6. K. Green and B. Krauskopf, "Bifurcation analysis of frequency locking in a semiconductor laser with phase-conjugate feedback," *Int. J. Bif. Chaos* **13**(9), pp. 2589–2601, 2003.
7. K. Green and B. Krauskopf, "Global bifurcations at the locking boundaries of a semiconductor laser with phase-conjugate feedback," *Phys. Rev. E* **66**(016220), 2002.
8. K. Green, B. Krauskopf, and K. Engelborghs, "Bistability and torus break-up in a semiconductor laser with phase-conjugate feedback," *Phys. D* **173**, pp. 114–129, 2002.
9. K. Green, B. Krauskopf, and G. Samaey, "A two-parameter study of the locking region of a semiconductor laser subject to phase-conjugate feedback," *SIAM J. Dynamical Systems* **2**(2), pp. 254–276, 2003.

10. R. Lang and K. Kobayashi, "External optical feedback effects on semiconductor injection laser properties," *IEEE J. Quantum Electron.* **16**(3), pp. 347–355, 1980.
11. O. Diekmann, S. A. Van Gils, S. M. V. Lunel, and H. O. Walther, *Delay Equations: Functional-, Complex-, and Nonlinear Analysis*, vol. 110, Springer-Verlag, 1995.
12. J. K. Hale and S. M. Verduyn Lunel, *Introduction to Functional Differential Equations*, Springer-Verlag, 1993.
13. S. M. Verduyn Lunel and B. Krauskopf, "The mathematics of delay equations with an application to the Lang-Kobayashi equations," in B. Krauskopf and D. Lenstra (Eds.), *Fundamental Issues of Nonlinear Laser Dynamics*, AIP Conference Proceedings **548**, pp. 66–86, 2000.
14. D. H. DeTienne, G. R. Gray, G. P. Agrawal, and D. Lenstra, "Semiconductor laser dynamics for feedback from a finite-penetration-depth phase-conjugate mirror," *IEEE J. Quantum Electron.* **33**, pp. 838–844, 1997.
15. O. K. Anderson, A. P. A. Fischer, I. C. Lane, E. Louvergneaux, S. Stolte, and D. Lenstra, "Experimental stability diagram of a diode laser subject to weak phase-conjugate feedback from a rubidium vapor cell," *IEEE J. Quantum Electron.* **35**, pp. 577–582, 1999.
16. K. Engelborghs, T. Luzyanina, and D. Roose, "Numerical bifurcation analysis of delay differential equations using DDE-BIFTOOL," *ACM Trans. Math. Softw.* **28**, pp. 1–21, 2002.
17. G. R. Gray, D. Huang, and G. P. Agrawal, "Chaotic dynamics of semiconductor lasers with phase-conjugate feedback," *Phys. Rev. A* **49**, pp. 2096–2105, 1994.
18. W. A. van der Graaf, L. Pesquera, and D. Lenstra, "Stability of a diode laser with phase-conjugate feedback," *Opt. Lett.* **23**(4), pp. 256–258, 1998.
19. W. A. van der Graaf, L. Pesquera, and D. Lenstra, "Stability and noise properties of diode lasers with phase-conjugate feedback," *IEEE J. Quantum Electron.* **37**(4), pp. 562–573, 2001.
20. B. Krauskopf, G. H. M. Van Tartwijk, and G. R. Gray, "Symmetry properties of lasers subject to optical feedback," *Opt. Commun.* **177**, pp. 347–353, 2000.
21. G. H. M. Van Tartwijk and G. P. Agrawal, "Laser instabilities: a modern perspective," *Prog. Quantum Electron.* **22**, pp. 43–122, 1998.
22. K. Green and B. Krauskopf, "Bifurcation analysis of a semiconductor laser subject to non-instantaneous phase-conjugate feedback," *Opt. Commun.*, **231**, pp. 383–393, 2004.